https://doi.org/10.5194/acp-2020-11
Preprint. Discussion started: 28 February 2020
© Author(s) 2020. CC BY 4.0 License.

Atmospheric Chemistry and Physics Discussions

Source characterization of volatile organic compounds measured by PTR-ToF-MS in Delhi, India

Liwei Wang[1], Jay G. Slowik[1], Nidhi Tripathi[2], Deepika Bhattu[1], Pragati Rai [1], Varun Kumar[1], Pawan Vats[4], Rangu Satish[5,a], Urs Baltensperger[1], Dilip Ganguly[4], Neeraj Rastogi[5], Lokesh K. Sahu[2], Sachchida N. Tripathi[3,*], and André S. H. Prévôt[1,*]

[1] Laboratory of Atmospheric Chemistry, Paul Scherrer Institute, Villigen, 5232, Switzerland

[2] Space and Atmospheric Sciences Division, Physical Research Laboratory, Ahmedabad 380009, India

[3] Department of Civil Engineering and Centre for Environmental Science and Engineering, Indian Institute of Technology Kanpur, Kanpur 208016, India

[4] Centre for Atmospheric Sciences, Indian Institute of Technology Delhi, New Delhi 110016, India

[5] Geosciences Division, Physical Research Laboratory, Ahmedabad 380009, India

[a] Now at: Department of Environmental Science and Analytical Chemistry, Stockholm University, Stockholm 11419, Sweden

[*] Corresponding authors

https://doi.org/10.5194/acp-2020-11
Preprint. Discussion started: 28 February 2020
© Author(s) 2020. CC BY 4.0 License.

Atmospheric Chemistry and Physics Discussions

Abstract. Characteristics and sources of volatile organic compounds (VOCs) were investigated with highly time-resolved simultaneous measurements by two proton-transfer-reaction time-of-flight mass spectrometers (PTR-ToF-MS) at an urban and a suburban site in New Delhi, India from January to March 2018. During the measurement period, high mixing ratios of VOCs and trace gases were observed, with high nocturnal mixing ratios and strong day-night variations. The positive matrix factorization (PMF) receptor model was applied separately to the two sites, and six major factors of VOCs were identified at both sites, i.e., two factors related to traffic emissions, two to solid fuel combustion, and two secondary factors. At the urban IITD site, traffic-related emissions comprising mostly mono-aromatic compounds were the dominant sources, contributing 56.6% of the total mixing ratio, compared to 36.0% at the suburban MRIU site. Emissions from various solid fuel combustion processes, particularly in the night, were identified as a significant source of aromatics, phenols and furans at both sites. The secondary factors accounted for 15.9% of the total VOC concentration at IITD and for 33.6% at MRIU. They were dominated by oxygenated VOCs and exhibited substantially higher contributions during daytime.

Key words: VOCs, Source apportionment, traffic emission, solid fuel combustion, secondary formation, Delhi

https://doi.org/10.5194/acp-2020-11
Preprint. Discussion started: 28 February 2020
© Author(s) 2020. CC BY 4.0 License.

Atmospheric Chemistry and Physics Discussions

1 Introduction

Volatile organic compounds (VOCs) are important trace gas constituents in the troposphere, impacting local and regional air quality, human health and climate both directly and indirectly (IPCC, 2013). With the participation of NO_x, oxidation of VOCs leads to the formation of tropospheric O_3, causing regional photochemical smog (Atkinson, 2000;de Gouw et al., 2005). The chemical transformation of VOCs forms less-volatile compounds and can contribute to new particle formation and fine particle growth via nucleation and partitioning (Hallquist et al., 2009; Ehn et al., 2014). In addition, many VOCs are toxic, such as aromatic compounds, and exposure to large amounts of VOCs may adversely affect human health, including acute and chronic effects on different systems and organs, and even cancer (Kampa and Castanas, 2008; Nurmatov et al., 2013).

VOCs originate from both natural and anthropogenic sources. Biogenic VOCs (BVOCs), mainly emitted by plants, are regarded as the largest natural source of VOCs globally (Atkinson and Arey, 2003; Hallquist et al., 2009). However, in urban areas, anthropogenic VOCs can be dominant (Borbon et al., 2013). Vehicular exhaust emissions have long been regarded as the dominant source of VOCs in many urban areas. Many of these compounds are reactive and thus contribute significantly to urban O_3 pollution, photochemical smog, and secondary organic aerosol (SOA) formation (Fraser et al., 1998; Derwent et al., 2010; Müller et al., 2012). Biomass burning is considered as the second largest source of VOCs worldwide (Crutzen and Andreae, 1990) and could be a major VOC source in some urban areas during biomass burning events (Karl et al., 2007; Yokelson et al., 2009; Baudic et al., 2016; Languille et al., 2019). Compared to vehicular emissions, biomass burning sources emit more oxygenated and high molecular-weight VOCs such as furans and phenols. Due to high atmospheric reactivity and higher SOA yield, these compounds can also contribute significantly to SOA formation.

Air pollution in South Asia has attracted more and more attention in recent years. This region is regarded as one of the most polluted regions in the world (e.g., Monks et al., 2009). Due to rapid urbanization and the lack of widespread advanced pollution control technologies in the industrial, energy, and transportation sectors (Mahata et al., 2018), air pollution has become an increasingly important issue across the region, particularly in large urban areas. The increasing emissions of air pollutants not only impact the local/regional air quality and human health, but also influences distant and pristine areas through transport (Bonasoni et al., 2010; Lawrence and Lelieveld, 2010; Mahata et al., 2018). Delhi, the capital city of India, with a population of 18.98 million (2012) people, is facing an air quality problem ranked as the worst among 1600 major cities in the world (WHO, 2014). The critical air quality problems have left India with high death rates from chronic obstructive pulmonary disease (COPD) and respiratory disease e.g., asthma. Despite the severe air pollution in Delhi, information on pollution levels, as well as an emission inventory of VOCs, and their sources in Delhi is still lacking (Monks et al., 2009; Kumar et al., 2015). A few studies on BTEX (i.e. benzene, toluene, ethylbenzene, and xylene) in Delhi reported that vehicular emissions could be the dominant source in Delhi (Srivastava et al., 2005; Hoque et al., 2008). Several studies also identified motor vehicle emissions as a significant source of particulate matter (PM), with high contributions from solid fuel combustion and industrial emissions (Sahu et al., 2011; Sharma et al., 2014; Kumar et al., 2015). These studies reveal the importance of local anthropogenic sources. However, since previous studies mainly focused on certain families of VOCs or a few VOCs species, a comprehensive

https://doi.org/10.5194/acp-2020-11
Preprint. Discussion started: 28 February 2020
© Author(s) 2020. CC BY 4.0 License.

Atmospheric Chemistry and Physics Discussions

investigation VOC pollution levels, specific emission sources, as well as their roles in the local tropospheric chemistry has not been reported previously. VOC source apportionment studies have been conducted only in a few Indian cities; for example, Srivastava studied 23 VOC compounds in Mumbai city, and illustrated the importance of evaporative and oceanic emissions (Srivastava, 2004). Sahu and Saxena (2015) studied 15 VOC species measured by a PTR-ToF-MS in urban Ahmedabad in winter. A recent study on 32 VOCs at Mohali (a suburban site in northwest Indo-Gangetic Plain) identified biofuel usage, biomass burning and vehicular emissions as important primary sources, and pointed out the lacking of present emission inventories (Pallavi et al., 2019).

In this study, we report simultaneous on-line measurements of VOCs using two PTR-ToF-MS instruments at an urban and a suburban site of Delhi, India. The level, composition and source characteristics of different VOCs were analyzed with the aid of the positive matrix factorization (PMF) model. Spatial and temporal comparisons between the two sites were discussed for both the sources and selected ions.

2 Experiments and methods

2.1 Measurement sites

Figure 1 shows the studied region and locations of the two measurement sites. The measurements were conducted from 18 January to 10 March 2018 at the Indian Institute of Technology (IITD), New Delhi, and from 16 January to 8 March 2018 at Manav Rachna International University (MRIU), Faridabad.

At the urban site (28° 33'N, 77° 12'E), the inlet system was installed on the rooftop (~20 m above the ground) of block VI (a four-story building), Centre for Atmospheric Sciences, on the campus of IITD (Gani et al., 2019). The IITD campus is located in the southern part of the city center, and is surrounded by educational, commercial, and residential districts. The study site is approximately 150 m north of a busy street and surrounded by several streets as well. Thus, in addition to vehicular emissions, commercial and residential activities may also produce VOC emissions in the immediate vicinity. The sampling line of the PTR-ToF-MS was approximately 1.5 m long, and the inlet consisted of polyether ether ketone (PEEK) tubing, with an inner diameter of 0.075 mm.

The other measurement site, at MRIU, was located in a relatively open area in suburban Delhi, about 20 km southeast of the IITD site. The site is located to the southeast of higher elevation terrain as shown in Figure 1. The suburban site is located inside a big campus, and it is surrounded by several small parks, with only a few narrow roads nearby. Although the site is not far from the main road, the traffic load and other anthropogenic activities nearby may be much less than that at IITD. The instruments were located on the first floor of a teaching building on the campus of MRIU. A similar PEEK inlet as at IITD was used, with the sampling line approximately 2 m long.

2.2 Online instruments

Data collected in this study included the mixing ratios of VOCs, NO_x, CO, and meteorological parameters. The involved monitors, analyzers, and sensors are described in detail below.

https://doi.org/10.5194/acp-2020-11
Preprint. Discussion started: 28 February 2020
© Author(s) 2020. CC BY 4.0 License.

Atmospheric Chemistry and Physics Discussions

In this campaign, two PTR-ToF-MS 8000 (Ionicon Analytical G.m.b.H, Innsbruck, Austria) were simultaneously deployed at the two sites. At both sites, the PTR-ToF-MS instruments were operated in the H_3O^+ mode, where the sampled VOCs are protonated via non-dissociative proton transfer from H_3O^+ ions (Eq.1):

$$H_3O^+ + R \rightarrow RH^+ + H_2O \quad (1)$$

The PTR-ToF-MS measures non-methane organic gases (NMOG) with a proton affinity higher than water, i.e., most of the common VOCs such as carbonyls, acids, and aromatic hydrocarbons, as well as alkanes with more than eight carbons and alkenes with more than two carbons. A detailed description of the instrument is found in Jordan et al. (2009) and Graus et al. (2010). For both sites, the time resolution was set to 30 s, the drift tube voltage was set at 600 V, with a drift temperature of 60 ºC, and a pressure of 2.2-2.3 mbar, resulting in an electric field (*E/N*) value of about 130 Td. Therefore, a similar fragmentation pattern is expected. Calibrations were performed twice at the IITD site and three times at the MRIU site by dynamic dilution of VOCs using a certified 15-compound gas standard (Ionimed Analytik GmbH, Austria at ~ 1 ppmv; with stated accuracy better than 8 %). The calibration components were methanol, acetonitrile, acetaldehyde, ethanol, acrolein, acetone, isoprene, crotonaldehyde, 2-butanone, benzene, toluene, o-xylene, chlorobenzene, α-pinene, and 1, 2-dichlorobenzene. The raw data were processed using the Tofware post processing software (version 2.5.11, TOFWERK AG, Thun, Switzerland) with the PTR module as distributed by Ionicon Analytik GmbH (Innsbruck, Austria), running in the Igor Pro 6.37 environment (Wavemetrics Inc., Lake Oswego, OR, U.S.A.). Mixing ratios (in ppbv) were calculated based on the method described by de Gouw and Warneke (2007) and the literature reaction rates (k) of the ion with the H_3O^+ ion were applied when available (Cappellin et al., 2012). For ions where the reaction rate had not been measured, a rate constant of 2×10^{-9} cm^3 s^{-1} was assumed.

The mixing ratio of NO_x was measured by chemiluminesence using the Serinus 40 Oxides of Nitrogen analyser (Ecotech) at IITD and a Model 42i (TEC, USA) at MRIU. The CO mixing ratio was analyzed with infrared radiation absorption method using a CO Analyzer (Serinus 30, Ecotech) at IITD and a Model 48i (TEC, USA) at MRIU.

2.3 Source apportionment

Source apportionment of VOCs was performed using the positive matrix factorization (PMF) receptor model (Paatero and Tapper, 1994), which represents the measured PTR-ToF-MS mass spectral time series as a linear combination of static factor profiles (characteristic of particular sources and/or atmospheric processes) and their time-dependent concentrations. This can be represented in matrix notation as follows:

$$\mathbf{X} = \mathbf{GF} + \mathbf{E} \quad (2)$$

Where **X**, **G**, **F**, and **E** are matrices corresponding to the measured mass spectral time series (time x *m/z*), factor time series (time x factor), factor profiles (factor x *m/z*), and model residuals (time x *m/z*), respectively. In this study, we used a total of 158 ions at IITD and 90 ions at MRIU measured by the PTR-ToF-MS (list of ions shown in Table S1 and Table S2). Equation (2) is solved by minimizing the objective function, Q (Eq. 3), using a weighted least-squares algorithm:

$$Q = \sum_i^n \sum_j^m \left(e_{ij}/s_{ij}\right)^2 \quad (3)$$

https://doi.org/10.5194/acp-2020-11
Preprint. Discussion started: 28 February 2020
© Author(s) 2020. CC BY 4.0 License.

Atmospheric Chemistry and Physics Discussions

Here, e_{ij} is the residuals (elements of **E**) and s_{ij} represents the corresponding measurement uncertainty.

As recommended by Paatero (2003), ions with a signal-to-noise ratio (SNR) lower than 0.2 were excluded from the input matrix, and ions with a signal-to-noise ratio (SNR) between 0.2 and 2 were down-weighted by increasing their uncertainties by a factor of 2. In addition, in this study, a few ions such as methanol, acetaldehyde, acetone, and acetic acid with extremely high mixing ratios were excluded from the input. Due to extremely high SNR compared to other compounds, inclusion of these ions in PMF leads to solution where only these ions are well-explained, and useful source information is not retrieved.

PMF was implemented as the Multilinear Engine (ME-2) (Paatero, 1999), with the Source Finder (SoFi) toolkit for Igor Pro (Wavemetrics, Inc., Portland; Canonaco et al., 2013) used for model configuration and post-analysis. As different combinations of **G** and **F** can yield mathematically similar solutions (i.e., similar *Q*), ME-2 enables intelligent rotational control to achieve reasonable solutions by involving constraints and external data. In this study, constraints were applied combining a scalar *a* (usually between 0 and 1) and a reference profile (Canonaco et al., 2013). The *a* value determines the extent to which the resolved factors *f'* and *g'* are allowed to vary from the input reference elements of *f* and *g* according to Eq. 4:

$$f' = f \pm a \cdot f \quad \text{and} \quad g' = g \pm a \cdot g \tag{4}$$

3 Results and discussion

3.1 Temporal and spatial variation

Figure 2 presents time series of the mixing ratios of CO and NO_x as well as of the sum of all VOCs analyzed in the PMF model and temperature at the two sites. The fractional composition of VOCs in terms of the chemical formula-derived families is included as well. The mean mixing ratios of CO were 1.29 ppmv, and 0.95 ppmv at IITD and MRIU, respectively. The average mixing ratios of NO_x at IITD was 148.0 ppbv, 5 times higher than at MRIU (29.6 ppbv). Similarly, the summed VOC mixing ratio (i.e., all the ions included in PMF analysis, see Table S1 and S2) was 27.6 ppbv at IITD, significantly higher than at MRIU (19.4 ppbv). The ambient temperature showed large variations during the campaign with an overall increasing trend after 21 February. Thus, the whole study period can be divided into two separate periods of relatively cold and warm temperatures. Figure S1 shows the average diurnal temperature patterns during the two periods. As shown in Figure S1, the mean temperature reached a minimum of 11 ºC at 7:00 LT and a maximum of 23 ºC at 14:00 LT during the cold period. During the warm period, the lowest and highest temperatures were 18 ºC at 6:00 LT and 32 ºC at 14:00 LT, respectively. These large differences in temperature along with other meteorological parameters are expected to have an impact on the emission profiles as well as the dilution and chemical transformation processes.

To investigate temporal and site-dependent changes in the relative composition of the VOCs, the measured signals of different ions were classified into seven families based on their identified chemical formula, namely aromatic C_xH_y, non-aromatic C_xH_y, $C_xH_yO_1$, $C_xH_yO_2$, $C_xH_yO_3$, C_xH_yN, and $C_xH_yNO_z$ compounds. Aromatic C_xH_y were classified due to their low H:C ratio, and oxidized aromatics are classified into the three $C_xH_yO_z$ families. Aromatic C_xH_y were the largest fraction at both sites constituting about 45.4% at IITD and 34.3% at

https://doi.org/10.5194/acp-2020-11
Preprint. Discussion started: 28 February 2020
© Author(s) 2020. CC BY 4.0 License.

Atmospheric Chemistry and Physics Discussions

MRIU. The high fractions of aromatic compounds indicate strong influences from anthropogenic emissions, mainly vehicle exhaust, at both sites. At IITD, the contributions of $C_xH_yO_1$ (21.9%) and $C_xH_yO_2$ (13.6%) were also significant, followed by non-aromatic C_xH_y (11.3%), C_xH_yN (5.2%), $C_xH_yO_3$ (2.3%), and C_xH_yNO (0.4%). At MRIU, the VOC family composition was similar, with the exception of a higher fraction of non-aromatic C_xH_y (23.2%), which was dominated by C_5H_8 and C_6H_{10}.

Owing to the variation of planetary boundary layer height (PBLH), as well as emission sources, temperature, and solar radiation, the time series of the mixing ratios of VOCs, NO_x and CO exhibited substantial differences between day and night periods. The nocturnal mixing ratios of the VOC sum, as well as of CO and NO_x were higher than during daytime, with much greater diurnal variation at IITD than at MRIU. The difference in diurnal variation may be due to a lower influence of local emissions at the suburban MRIU site because of lower population density and fuel consumption. In addition, the relative proportions of the VOC families varied over time, indicating different emission patterns and oxidation chemistry. For instance, substantial aromatic contributions were observed at night, indicating strong anthropogenic emissions in the urban area, such as traffic related emissions and solid fuel combustion. Meanwhile, higher daytime contributions were found for the $C_xH_yO_1$ and $C_xH_yO_2$ compounds, indicating tropospheric aging and secondary formation during daytime.

3.2 VOC source apportionment

3.2.1 Solution selection

We evaluated unconstrained solutions from 4-11 factors individually for both sites, and solutions were selected based on interpretation of the spectra, reference information from emission inventory, correlation of VOC factors with ancillary measurements, and mathematical diagnostics describing PMF performance. A six-factor solution was selected as the best representation of the data measured at both sites, which includes two traffic factors, two solid fuel combustion factors, and two secondary factors. An industrial factor is not presented in the result, as marker compounds typically originating from industrial emissions are either not measured (such as halogen compounds) nor included in the PMF analysis (such as methanol and acetone as described in Section 2.3). In terms of PMF performance, the Q/Q_{exp} did not show any step change with increasing factor number (Fig. S2). Solutions with less than six factors failed to provide reasonably separated sources, while solutions with more factors led to additional traffic or solid fuel combustion factors that did not improve the interpretability of the results. These additional factors were likely the result of minor variations across discrete instances of a given source (e.g. vehicle-to-vehicle variations in VOC composition) and slight differences in reactive history.

At IITD, due to very high concentrations of several aromatics measured, initial PMF results were over-weighted towards explaining aromatic variability, with the result that aromatics were apportioned to all the resolved factors, including factors that otherwise appear secondary and where such attribution is not reasonable. To this mathematical artifact and guide the model towards environmentally reasonable results, constraints were applied to the IITD secondary factors as follows. First, PMF was performed with a new input matrix excluding the most abundant aromatic ions, namely $C_6H_6H^+$, $C_7H_8H^+$, $C_8H_{10}H^+$, and $C_9H_{12}H^+$ (PMF results with the new input are shown in Fig. S3). This yielded a reasonable five-factor solution was resolved, from which the spectra of the two secondary factors were selected for use as reference profiles in the original dataset. PMF was then executed

https://doi.org/10.5194/acp-2020-11
Preprint. Discussion started: 28 February 2020
© Author(s) 2020. CC BY 4.0 License.

Atmospheric Chemistry and Physics Discussions

again on the full dataset (i.e., all 158 ions including the aromatics), with constraints applied to the two secondary factors using the *a*-value approach. Since we obtained the reference from the same dataset, the *a*-value was set to a smaller range than the usual case. Here, solutions with the *a*-value ranging from 0.1 to 0.3 were evaluated and no significant differences in terms of the spectra and temporal variations were observed among all the results. In the following analysis, the solution with an *a*-value=0.1 for both factors was selected as the IITD result, and the averaged result with the *a* value range from 0.1-0.3 are presented in Figure S4.

At MRIU, the lower aromatic concentrations meant that that even the unconstrained PMF did not apportion significant aromatic mass to resolved secondary factors. For consistency, we tested also the constraint-based method described above, but the two methods did not yield significant differences at MRIU (see Figure S5). Therefore, at MRIU the unconstrained solution was selected for further interpretation.

3.2.2 Factor identification

Figures 3 and 4 show the factor profiles (a), time series (b), and diurnal patterns (c) of the selected PMF solution at IITD and MRIU, respectively. In the following, we present a detailed discussion of the factor characteristics at IITD. The MRIU factors are qualitatively similar and therefore a detailed discussion is not repeated, but rather a site comparison is presented in Section 3.3.

The first two factors are related to vehicle emissions and denoted Traffic1 and Traffic2. Both are enhanced during the night and relatively low during daytime. The mass spectra of both Traffic1 and Traffic2 are dominated by aromatic C_xH_y compounds, namely C_6H_6, C_7H_8, C_8H_{10}, C_9H_{12}, and $C_{10}H_{14}$. These ions are tentatively attributed to benzene, toluene, C8-aromatics, C9-aromatics, and C10-aromatics, which are well-studied markers for vehicular emissions (Yao et al., 2015; Cao et al., 2016). While Traffic1 is mostly composed of pure aromatics, Traffic2 includes relatively high contributions from non-aromatic hydrocarbons and some oxygenated compounds. As shown in Fig. 3 (b), both traffic factors exhibit temporal variations similar to NO_x, which originates mainly from vehicle emissions in an urban area. To alleviate urban traffic congestion, heavy-duty vehicles are banned in Delhi during the rush hours (7:00-10:00 LT and 17:00-21:00 LT). As a result, most heavy-duty traffic in Delhi occur overnight rather than during daytime. This difference in traffic patterns corresponds to the temporal differences in Traffic1 and Traffic2. Specifically, Traffic2 is an important source from 21:00 LT to 7:00 LT the next morning, while Traffic1 is higher during daytime, in particular in the morning rush hour period and even around noon, consistent with local traffic patterns of passenger vehicles. Therefore, Traffic1 is identified as more influenced by light-duty vehicle emissions and Traffic2 to be more influenced by heavy-duty vehicles. Since the vehicle number in Delhi has increased dramatically in the past two decades, related pollution is considered as an increasingly significant source of atmospheric pollution. Overall, the sum of the two traffic factors is found to be the dominant VOC source in Delhi, with contributions of 33.8% from Traffic1 and 22.8% from Traffic2 to the total analyzed VOCs.

Two other factors are found to be related to solid fuel combustion (SFC) and are named as SFC1 and SFC2. SFC1 is characterized by high loadings of aromatics, as well as oxygenated ions, such as $C_6H_6(C_nH_{2n})O_1$, $C_6H_6(C_nH_{2n})O_2$, $C_4H_4(C_nH_{2n})O_1$, $C_4H_4(C_nH_{2n})O_2$, and $C_5H_4O_{1\text{-}2}$. These ions are tentatively attributed to phenolic compounds and furans. Previous studies have reported that furans and phenols are emitted in high quantities by

https://doi.org/10.5194/acp-2020-11
Preprint. Discussion started: 28 February 2020
© Author(s) 2020. CC BY 4.0 License.

Atmospheric Chemistry and Physics Discussions

wood/biomass burning and coal combustion (Bruns et al., 2017; Klein et al., 2018) and thus are regarded as important markers for these combustion processes. In urban Delhi, the use of solid fuels is not limited to wood and coal, but includes open combustion of many types of biomass and even waste. In addition, traditional stoves remain popular in some residential households and restaurants, and their VOC emission profiles are still not clear. SFC1 is identified as being more related to primary emissions from solid fuel combustion, which might include many types of biomass burning, coal combustion, and even trash combustion. The spectrum of the SFC2 factor is dominated by benzene and to a lesser extent toluene, while the more reactive phenols and furans are only present in small amounts, suggesting increased age. In addition, it includes a high mass fraction of N-containing compounds, such as C_3H_3N, C_4H_5N, and C_7H_5N. Although the chemical identification of these ions is not confirmed, these ions were reported in biomass burning as well (Stockwell et al., 2015; Sekimoto et al., 2018) and may be attributed to nitriles, which have longer OH lifetimes compared to furans and phenols (Meylan and Howard, 1993; Atkinson et al., 1989). SFC2 also explains a higher fraction of higher molecular-weight molecules, e.g. $C_6H_5NO_3$ and $C_7H_7NO_3$. These ions are attributed to nitrophenols, which are semivolatile compounds found in biomass burning-related secondary organic aerosol (Mohr et al., 2013). As shown in Fig 3(c), SFC1 exhibits a diurnal pattern with a maximum value at 20:00 LT and a smaller peak at 8:00 LT in the morning hours, consistent with residential heating and/or cooking activities. SFC2 is also high at night, although it peaks several hours later than SFC1 (at 5:00 LT), and decreases strongly during daytime without any morning peak. This suggests that the nocturnal peak of SFC2 may be due to dark oxidation of emitted precursor VOCs, e.g. by nitrate radicals. Therefore, considering emissions, chemical transformation and reactivity, SFC1 represents more primary emissions from various types of solid fuel combustion in central Delhi, while SFC2 is associated with more aged emissions from solid fuel combustion.

Finally, two secondary VOC factors are identified, the spectra of which are distinguished from the other factors by a strong presence of oxygenated compounds. Secondary VOC1 (denoted SecVOC1 in the following) contributes a large fraction of $C_2H_4O_3$ and $C_4H_2O_3$, and the spectrum is dominated by C_4H_8O, $C_3H_4O_2$, $C_3H_6O_2$, and $C_3H_6O_3$, although the relative contributions to these ions are comparably lower than to $C_2H_4O_3$ and $C_4H_2O_3$. These ions are likely oxidation products from various photochemical processes and are not unique to specific precursors and oxidation processes. However, many of these ions can be formed rapidly during daytime and may have a short lifetime owing to partitioning to the condensed phase and/or heterogeneous processes. The time series of SecVOC1 follows that of solar radiation, which has a regular contribution cycle during daytime, with a rapid enhancement starting from around 7:00-8:00 LT. Secondary VOC2 (SecVOC2) has significant contributions from $C_3H_4O_2$ and $C_3H_6O_2$ as well, but the relative contributions to $C_3H_4O_2$, $C_4H_6O_{2\text{-}3}$, $C_6H_6O_2$, $C_8H_8O_3$, and $C_6H_5NO_3$ are substantially higher than by SecVOC1. It also includes many oxygenated compounds with higher molecular weight, e.g. $C_5H_{10}O_{1\text{-}2}$, $C_6H_{10}O_{1\text{-}2}$, and $C_6H_{12}O_{1\text{-}2}$. SecVOC2 (Fig. 3(c)) is not only high during daytime, with a slow rise in the morning and a peak around 10:00-12:00 LT, but is also high at night, reaching its nocturnal maximum from 20:00 LT to midnight. Major fractions of alkyl nitrates ($RONO_2$) are detected as ($ROH{\cdot}H^+$) fragment ions by the PTR-ToF-MS. Therefore, species such as $C_5H_{10}O_{1\text{-}2}$, $C_6H_{10}O_{1\text{-}2}$, and $C_6H_{12}O_{1\text{-}2}$, may be partially attributed to fragments from organic nitrates, which contribute to the high nocturnal SecVOC2 mixing ratio. Therefore, it is likely that SecVOC1 is a mix of first generation products and later-

https://doi.org/10.5194/acp-2020-11
Preprint. Discussion started: 28 February 2020
© Author(s) 2020. CC BY 4.0 License.

Atmospheric Chemistry and Physics Discussions

generation oxidation products, while SecVOC2 is possibly associated with secondary generation products and nighttime chemistry.

3.3 Comparison of VOC sources

Figure 5 compares the diurnal cycles and mass spectra of the two Traffic and the two SFC factors between the two sites. While the factor profiles are similar for the primary factors (i.e. Traffic1, Traffic 2 and SFC1) their diurnal patterns are very different. Higher nocturnal concentrations and day-night variations are observed at IITD than at MRIU for all three primary factors. For example, for Traffic1 the nocturnal maximum is 5.3 times higher than the daytime minimum at IITD and only 2.7 times higher at MRIU. For SFC1, the corresponding numbers are 36.8 at IITD and 6.9 at MRIU. This is possibly owing to increased traffic density and more intense combustion activities in the populated urban areas.

Unlike the primary factors, the mass spectra of SFC2 differ between the two sites. At IITD, SFC2 is not only rich in benzene, but also in toluene. However, as shown in Fig. 5, toluene is much lower at MRIU, while the relative benzene concentration remains high. In addition, SFC2 at MRIU is richer in some oxygenated compounds, such as $C_6H_{12}O_{1\text{-}2}$, $C_5H_{10}O_2$, $C_6H_{10}O_2$, $C_4H_{4/6/8}O_2$. These ions are the major ions found in the SecVOC2 factor at IITD. Because toluene has a much shorter photochemical lifetime than benzene, this suggests that SFC2 comprises less freshly emitted but more aged compounds at MRIU than at IITD. Although the SFC2 factors exhibit similar diurnal trends at the two sites, the time of daily maximum is different. At MRIU, SFC2 reaches the maximum at 7:00 LT, which is approximately 2 hours later than that at IITD. Further, the maximum averaged SFC2 mixing ratio at MRIU is 4.41 ppbv, lower than the peak value of 6.20 ppbv at IITD, and consistent with the higher primary emission levels at IITD.

The two secondary VOC factors, in particular, show major differences between the two locations in terms of diurnal variations and spectra. On a simple level, the two SecVOC2 are considered to represent the same factor because of their similar long-term trends with local temperature (Fig. 3 and 4). However, the mass spectra are very different, indicating different aging mechanisms. As illustrated in Fig. 3 and 4, the spectrum of SecVOC1 is dominated by $C_4H_2O_3$ and $C_2H_4O_3$ at IITD but less so at MRIU, especially in the case of $C_4H_2O_3$. On one hand, as shown in Fig. 6, the MRIU SecVOC1 is comparable to SecVOC2 at IITD in terms of factor fingerprint. The spectra of the two factors are both characterized by high contributions to $C_3H_4O_2$, $C_4H_6O_{2\text{-}3}$, $C_5H_{10}O_{1\text{-}2}$, $C_6H_{10}O_{1\text{-}2}$, and $C_6H_{12}O_{1\text{-}2}$, with a relatively higher contribution to $C_4H_2O_3$ and $C_2H_4O_3$ by MRIU SecVOC2. However, their time trends and diurnal variations are rather different. Although they both increase during daytime, the maximum is found about 4 hours later at MRIU than at IITD, possibly owing to less primary emission in the morning. Besides, the elevated periods of IITD SecVOC2 are not only related to higher temperature, but also consistent with the periods with much stronger primary emissions (e.g. Traffic factors). Similarly, the time series of MRIU SecVOC1 is also high in January when all the primary factors are high compared to the rest of the periods. Therefore, it is possible that MRIU SecVOC2 indicates the local oxidation processes as presented by both SecVOC factors at IITD. On the other hand, the spectrum of MRIU SecVOC2 is also loaded with $C_4H_2O_3$, $C_2H_4O_3$, as well as high C_4H_8O and $C_3H_4O_2$, but the contributions to these ions are much lower than SecVOC1. In addition, MRIU SecVOC2 exhibits a similar time series as that of local temperature, which increases in the warmer period of the campaign. The overall trend is quite different from the

https://doi.org/10.5194/acp-2020-11
Preprint. Discussion started: 28 February 2020
© Author(s) 2020. CC BY 4.0 License.

Atmospheric Chemistry and Physics Discussions

local primary factors, but has some similarities with that of IITD SecVOC2. Therefore, it is possible that MRIU SecVOC2 represents the oxidized VOCs on a relatively regional scale.

Figure 7 presents the stacked factor diurnal patterns at the two sites. Much higher nocturnal mixing ratios of VOCs are observed at IITD than at MRIU, leading to pronounced day-night differences, while during daytime higher mixing ratios are found at MRIU than at IITD (with 15 ppbv at MRIU in the mid-afternoon, compared to 10 ppbv at IITD). This can be explained by the fact that at IITD the VOC mixing ratio is dominated by primary emissions, especially during the night, while at MRIU the VOC mixing ratio is dominated by secondary formation, at least during the day. At IITD, primary factors contribute to around 85% before midnight, with large fractions coming from Traffic factors and SFC1. Afterwards, SFC2 gradually increases and contributes to over 40% of the total mixing ratio before sunrise, when other primary factors decrease to about 50%. At the suburban MRIU site, although the nocturnal mixing ratio of primary VOCs are about half as high as that at IITD, they contribute to around 70% of the total VOCs concentrations. In the daytime, however, the SecVOC contribution is as high as 54%, compared to the maximum 41% at IITD. Generally, the MRIU SecVOC contributes about 15-20% more than that at the IITD site throughout the day, mostly due to increased SecVOC1. This may be partially explained by the differences in rotation techniques we applied in running the model for both the secondary factors. As illustrated in Figure S6, by applying the similar *a*-value approach to MRIU as used at IITD, the constrained MRIU SecVOC is around 1.5 ppb lower than the raw PMF result, and contributes a maximum 10% less at around 14:00-15:00 LT. However, SecVOC contributes 31% to the total analyzed VOCs mixing ratio in the constrained MRIU solution, instead of a contribution of 34% from the unconstrained result as illustrated above. Both PMF solutions resolved at MRIU show much higher fractions of SecVOC compared to that at IITD (16%). Therefore, the rotation techniques only play a minor part on the discrepancies between the two sites. But more importantly, differences in SecVOC is probably owing to that chemical oxidation of primary VOCs occur to a larger extent downwind of urban emission sources instead of in the city, due to suppression of oxidants like OH radicals and longer oxidation time.

3.4 Evaluation of biogenic signatures

Biogenic VOCs, i.e. isoprene and monoterpenes, are not separated into a specific factor in this study. This is in part due to the small number of ions that can be unambiguously assigned to these sources. Specifically, the structure assignment and quantification of non-aromatic C_xH_y can be uncertain not only because of isomers, but also because of fragments from aldehydes, alcohol, and other long-chain aliphatic hydrocarbons. Therefore, C_5H_8 and the sum of $C_{10}H_{16}$ and C_6H_8 (a major fragment of $C_{10}H_{16}$) can only serve as upper estimates of the actual isoprene and monoterpenes, respectively. The averaged concentrations of isoprene and monoterpenes are very low during the campaign, with 0.8 ppbv and 0.46 ppbv, respectively at IITD, and 1.2 ppbv and 0.32 ppbv, respectively at MRIU. Figure 8 illustrates the explained variation of the two major biogenic markers (i.e. isoprene and monoterpenes) and several other ions possibly related to their oxidation products. Among them, $C_4H_6O_{1\text{-}2}$ and $C_4H_6O_{1\text{-}2}$ are found in photooxidation of isoprene, and $C_9H_{14}O$ and $C_{10}H_{14/16}O$ are potential photochemical products from monoterpenes. Instead of being related to a specific secondary factor, the biogenic markers are largely explained by primary factors. There are several possible explanations. First, both isoprene and monoterpenes have been found in biomass burning emissions from numerous laboratory and field studies

https://doi.org/10.5194/acp-2020-11
Preprint. Discussion started: 28 February 2020
© Author(s) 2020. CC BY 4.0 License.

Atmospheric Chemistry and Physics Discussions

(e.g. Bruns et al., 2017). Second, previous studies also indicated anthropogenic sources of isoprene from vehicular emissions (Borbon et al., 2001;Wagner and Kuttler, 2014). Third, considerable amounts of these ions may be affected by isomers and fragments of larger ions originating from primary emissions. Finally, the two BVOCs are very reactive compounds, which have very short lifetimes especially during daytime, and during nighttime only if NO_3 is present. Therefore, large amounts of BVOCs can be degraded very quickly via photochemical oxidation during daytime, resulting in lower daytime BVOC concentrations in despite of stronger natural emissions. As shown in Figure S7, both isoprene and monoterpene are high at night and very low during daytime, similar to the diurnal trends of primary factors. The only exception is isoprene at MRIU, which may be due to strong daytime emissions or contributions from isomers/fragments. Therefore, it is likely that the high observed nocturnal BVOC concentrations are due to primary emissions as suggested by the model.

As shown in Figure 8, the $C_xH_yO_z$ ions are explained partially by secondary factors, indicating possible secondary formation from biogenic precursors. However, at both sites, considerable amounts of these ions are also explained by emissions from SFC. It is consistent with the results that these oxygenated ions were found in biomass/wood burning emissions as shown in previous studies (Bruns et al., 2017; Koss et al., 2018). Besides, as these small molecular weight ions are possible products from various precursors and chemical pathways, their structures and precursor definitions are uncertain. However, the explained variations can still provide information on the aging processes. In general, the fraction explained by secondary factors increases as the ions become more oxygenated. In addition, at IITD SecVOC1 explains much higher fractions of the $C_xH_yO_1$ ions compared to SecVOC2, while the $C_xH_yO_{2\text{-}3}$ ions are to a great extent explained by SecVOC2. As some of these less oxygenated ions originate from both fast photochemical formation and later-generation production, they are explained by both secondary factors. For example C_4H_6O, which can be attributed to MVK and MACR, is formed rapidly via isoprene OH oxidation, by also be found as the secondary generation products via several other oxidation pathways. Generally, both biogenic markers and their oxidation products are low during the measurement period, and these ions contribute only small amounts to the two secondary factors, indicating minor contributions from biogenic emissions at the two sites during the campaign.

3.5 Characteristics of selected ions

Figure 9 shows the diurnal patterns of the explained variation of each PMF factor to selected ions measured at the two sites, stacked such that the height is the total modelled concentration. The red line in each plot represents the mean diurnal pattern of the measured mixing ratio. The model represents over 80% of most of these selected ions, and thus in general explains the variations of these ions well. The comparison of these diurnal patterns illustrates that distinct differences exist in the concentrations, variations, and source compositions of certain VOCs. The assignment of a specific compound structure to each ion can be ambiguous, particularly for the spectra obtained from ambient air due to the possibility of isomers and/or fragmentation. Still, we provide tentative candidates for the nine ions based on their molecular formulas and compounds found in previous fuel combustion and oxidation simulation studies. Structural assignments for aromatics and PAHs are more certain because the low H to C atomic ratio reduces the number of reasonable structures, therefore, C_6H_6, C_7H_8 and $C_{10}H_8$ are mainly attributed to benzene, toluene, and naphthalene, respectively. Also included in Fig. 9 are $C_5H_4O_2$, C_6H_6O, $C_2H_4O_3$, $C_4H_2O_3$, and $C_6H_5NO_3$; we suggest that the most likely structural

https://doi.org/10.5194/acp-2020-11
Preprint. Discussion started: 28 February 2020
© Author(s) 2020. CC BY 4.0 License.

Atmospheric Chemistry and Physics Discussions

assignments are furfural, phenol, a fragment of peroxyacetyl nitrate (PAN), maleic anhydride, and nitrophenol, respectively.

Benzene and toluene are well-interpreted aromatics, which contribute significantly to emissions from several combustion processes, including vehicle emissions, biomass burning, coal combustion, etc. (Pieber et al., 2018; Bruns et al., 2017; Klein et al., 2018). As shown in Fig. 9 (a), at IITD benzene originates to a significant extent from traffic emissions over the whole day and in addition from SFC factors at night. This suggests that the IITD site is dominated by pollution from vehicular emissions because of the highly trafficked streets nearby, and also influenced by strong solid fuel combustion due to the high population density. At MRIU, however, there are comparable benzene contributions by the Traffic1, SFC1, and SFC2 factors. Even though the sum of the SFC mixing ratios is lower at MRIU compared to IITD, the relative SFC contribution is higher at MRIU. Toluene displays a similar diurnal cycle and source contributions as benzene, characterized by significant contributions from primary sources, especially Traffic1.

As mentioned above, phenolic compounds and substituted furans are found to be significant oxygen-containing compounds at the two sites. Furfural is an important marker from biomass burning, which arises from pyrolysis of cellulose and hemicellulose. Phenols are detected in biomass burning and coal combustion emissions as the most abundant oxygenated aromatic compounds. (Stockwell et al., 2015; Klein et al., 2018; Bruns et al., 2017) Indeed, as shown in Fig. 9 (c,f), the majority of furfural and phenol are explained by the two SFC factors at both sites. SFC1 contributes mainly during the night and morning, with a higher night-to-day ratio at IITD, which captures both the characteristics of residential heating styles and urban/suburban usage differences due to population density. The SFC2-to-SFC1 ratio generally increases during the night. As described earlier, one possible explanation is that SFC2 results from the fast nocturnal evolution of primary SFC1 emissions probably driven by night chemistry under high NO_x conditions (Tiitta et al., 2016). In addition to the SFC factors, at IITD around 8% of furfural and 4% of phenol are explained by the two SecVOC factors, compared to around 11% and 25% at MRIU, respectively.

Nitrated phenols are important biomass burning tracers, in particular for secondary aerosol formation (Mohr et al., 2013; Bertrand et al., 2018). Here, the diurnal cycles of $C_6H_5NO_3$ at the two sites illustrate contributions from both emission and atmospheric transformation. At both sites, SFC2 accounts for a large percentage of the nocturnal nitrophenol mixing ratios and the SecVOC factors explain the remaining fraction. This is consistent with SFC2 representing nighttime aging of SFC emissions. It is worth noting that during the night there is a much larger unexplained fraction (around 35%) at IITD than at MRIU, with a corresponding uncertainty in the source contributions. Still, the main difference at the two sites relate to the contributions of the SecVOC factors. At IITD, the SecVOC2 factor contributes more at night than during daytime, probably due to nocturnal formation including NO_3 chemistry and the photolysis reactions of $C_6H_5NO_3$ during daytime. At MRIU, both SecVOC1 and SecVOC2 contribute to $C_6H_5NO_3$, indicating the combined influences from local and regional chemistry.

Maleic anhydride and PAN display distinct variation patterns at the two sites. Maleic anhydride is the product from the photo-oxidation of furans, unsaturated carbonyls, and aromatics (Bierbach et al., 1994; Yuan et al., 2017). The mixing ratio of maleic anhydride is about 5 times higher at IITD than that at MRIU during daytime

https://doi.org/10.5194/acp-2020-11
Preprint. Discussion started: 28 February 2020
© Author(s) 2020. CC BY 4.0 License.

Atmospheric Chemistry and Physics Discussions

and is only explained by SecVOC1, indicating significant formation from the abundant emissions of VOC precursors and NO_x. During nighttime, the maleic anhydride mixing ratio at MRIU is similar to the one at IITD, with considerable amounts explained by SecVOC2 and SFC2. A recent study indicates that furans contributed to over 90% of maleic anhydride within the first 4 hours of OH oxidation in biomass burning plumes (Coggon et al., 2019). Therefore, the higher morning peak and nocturnal mixing ratios of furans may be the driver of much higher maleic anhydride at IITD. Besides, it is possible that under the conditions of high humidity and aerosol mass loading, maleic anhydride could react and/or condense away before the city plume reaching the suburban area. In contrast to maleic anhydride, $C_2H_4O_3$ shows a higher mixing at MRIU than at IITD. $C_2H_4O_3$ is mainly attributed to a fragment of PAN, however, a small fraction is also related to primary factors at both sites (Fig. 9). This ion was reported in laboratory studies on primary biomass burning emissions (Bruns et al., 2017). Possibly, small amounts of this ion might be attributed to unknown isomers, which are directly emitted or rapidly formed in combustion processes. PAN is formed in VOC oxidation with NO_x (de Gouw and Warneke, 2007). Due to its long lifetime at low temperature, PAN can undergo long-range transport and then play an important role in tropospheric ozone formation in the remote areas when it decomposes (Fischer et al., 2014). Here, PAN is mainly explained by SecVOC1 at IITD, suggesting local formation through the oxidation of abundant VOC precursors. In the rural area at MRIU, however, a much higher PAN mixing ratio is observed, originating from both secondary VOC factors, indicating a longer oxidation time at this site.

4 Conclusion

Measurements of volatile organic compounds (VOCs) were performed simultaneously at two different sites in Delhi, India using two PTR-ToF-MS instruments. Much higher mixing ratios of VOCs were observed at the urban IITD site, with higher nocturnal contributions from anthropogenic emissions than at the suburban MRIU site. Using positive matrix factorization, we found a 6-factor solution at both sites, each consisting of two traffic factors, two solid fuel combustion factors, and two secondary factors. Anthropogenic activities were shown to be important VOCs sources at both sites. Among them, traffic related emissions comprised the dominant source, contributing 56.6% at the urban IITD site and 36.0% at the suburban MRIU site to the total analyzed VOC mixing ratio (excluding high-intensity VOCs as described in Section 2.3. Solid fuel combustion contributed 27.5% at the urban IITD site, and even 30.4% at the suburban MRIU site. Secondary formation was the most important source of VOCs during daytime, and contributed 15.9% at IITD and 33.6% at MRIU to the total concentration. Higher concentrations of oxygenated VOCs were found at the suburban site, likely due to suppression of oxidant levels in the urban atmosphere and longer aging time at the suburban site.

Comparison of the factor diurnals and profiles indicated that the anthropogenic sources were similar at two sites, even though the VOC mixing ratios at MRIU were much lower than IITD. The secondary factors, however, were different at the two sites both in terms of diurnal variations and of spectra. The two secondary VOC factors exhibited higher mixing ratios and contributions at the suburban site, in particular during daytime. At IITD, the two SecVOC factors indicated different aging process under strong primary emissions, while at the suburban MRIU they suggested local oxidation and regional aging. Besides, evaluation of biogenic markers indicated very small influence from biogenic emissions and their oxidation products.

https://doi.org/10.5194/acp-2020-11
Preprint. Discussion started: 28 February 2020
© Author(s) 2020. CC BY 4.0 License.

Atmospheric Chemistry and Physics Discussions

This work highlights the crucial role that anthropogenic sources play in the pollution levels and variation characteristics of VOCs in the ambient atmosphere of Delhi, India. Further control measures to reduce emissions from traffic exhaust and solid fuel combustion are urgently needed to mitigate the severe pollution and the environmental impact of VOCs as well as aerosols (not investigated in this paper) in this region. Significant differences in the concentrations as well as the pollution sources stress the complexity of both emission and chemistry in this region. Long-term measurements of a set of VOCs, aerosols, and other oxidants would be ideal to obtain a more detailed understanding of the formation mechanisms during various conditions.

Data availability

Date will be available in ACP version.

Acknowledgement

This work was supported by the SNF projects 200021_169787 (SAOPSOAG), BSSGI0_155846 (IPR-SHOP), IZLCZ2_169986 (HAZECHINA), and 200021_162448/1 (China-XRF). SNT gratefully acknowledges the financial support provided by the Department of Biotechnology (DBT), Government of India to conduct this research under grant no. BT/IN/UK/APHH/41/KB/2016-17 dated 19th July 2017 and financial support provided by the Central Pollution Control Board (CPCB), Government of India to conduct this research under grant no. AQM/Source apportionment_EPC Project/2017.

https://doi.org/10.5194/acp-2020-11
Preprint. Discussion started: 28 February 2020
© Author(s) 2020. CC BY 4.0 License.

Atmospheric Chemistry and Physics Discussions

Reference

Atkinson, R., Baulch, D. L., Cox, R. A., Jr., R. F. H., Kerr, J. A., and Troe, J.: Evaluated kinetic and Photochemical Data for Atmospheric Chemistry: Supplement III. IUPAC Subcommittee on Gas Kinetic Data Evaluation for Atmospheric Chemistry, Journal of Physical and Chemical Reference Data, 18, 881-1097, 10.1063/1.555832, 1989.

Atkinson, R.: Atmospheric chemistry of VOCs and NOx, Atmospheric Environment, 34, 2063-2101, https://doi.org/10.1016/S1352-2310(99)00460-4, 2000.

Atkinson, R., and Arey, J.: Atmospheric degradation of volatile organic compounds, Chemical reviews, 103, 4605-4638, 2003.

Baudic, A., Gros, V., Sauvage, S., Locoge, N., Sanchez, O., Sarda-Estève, R., Kalogridis, C., Petit, J. E., Bonnaire, N., Baisnée, D., Favez, O., Albinet, A., Sciare, J., and Bonsang, B.: Seasonal variability and source apportionment of volatile organic compounds (VOCs) in the Paris megacity (France), Atmos. Chem. Phys., 16, 11961-11989, 10.5194/acp-16-11961-2016, 2016.

Bertrand, A., Stefenelli, G., Jen, C. N., Pieber, S. M., Bruns, E. A., Ni, H. Y., Temime-Roussel, B., Slowik, J. G., Goldstein, A. H., El Haddad, I., Baltensperger, U., Prevot, A. S. H., Wortham, H., and Marchand, N.: Evolution of the chemical fingerprint of biomass burning organic aerosol during aging, Atmos. Chem. Phys., 10, 7607-7624, 10.5194/acp-18-7607-2018, 2018.

Bierbach, A., Barnes, I., Becker, K. H., and Wiesen, E.: Atmospheric Chemistry of Unsaturated Carbonyls: Butenedial, 4-Oxo-2-pentenal, 3-Hexene-2,5-dione, Maleic Anhydride, 3H-Furan-2-one, and 5-Methyl-3H-furan-2-one, Environmental Science & Technology, 28, 715-729, 10.1021/es00053a028, 1994.

Bonasoni, P., Laj, P., Marinoni, A., Sprenger, M., Angelini, F., Arduini, J., Bonafè, U., Calzolari, F., Colombo, T., Decesari, S., Di Biagio, C., di Sarra, A. G., Evangelisti, F., Duchi, R., Facchini, M. C., Fuzzi, S., Gobbi, G. P., Maione, M., Panday, A., Roccato, F., Sellegri, K., Venzac, H., Verza, G. P., Villani, P., Vuillermoz, E., and Cristofanelli, P.: Atmospheric brown clouds in the Himalayas: first two years of continuous observations at the Nepal Climate Observatory-Pyramid (5079 m), Atmos. Chem. Phys., 10, 7515-7531, 10.5194/acp-10-7515-2010, 2010.

Borbon, A., Fontaine, H., Veillerot, M., Locoge, N., Galloo, J. C., and Guillermo, R.: An investigation into the traffic-related fraction of isoprene at an urban location, Atmospheric Environment, 35, 3749-3760, https://doi.org/10.1016/S1352-2310(01)00170-4, 2001.

Borbon, A., Gilman, J. B., Kuster, W. C., Grand, N., Chevaillier, S., Colomb, A., Dolgorouky, C., Gros, V., Lopez, M., Sarda-Esteve, R., Holloway, J., Stutz, J., Petetin, H., McKeen, S., Beekmann, M., Warneke, C., Parrish, D. D., and de Gouw, J. A.: Emission ratios of anthropogenic volatile organic compounds in northern mid-latitude megacities: Observations versus emission inventories in Los Angeles and Paris, Journal of Geophysical Research: Atmospheres, 118, 2041-2057, 10.1002/jgrd.50059, 2013.

Bruns, E. A., Slowik, J. G., El Haddad, I., Kilic, D., Klein, F., Dommen, J., Temime-Roussel, B., Marchand, N., Baltensperger, U., and Prévôt, A. S. H.: Characterization of gas-phase organics using proton transfer reaction time-of-flight mass spectrometry: fresh and aged residential wood combustion emissions, Atmos. Chem. Phys., 17, 705-720, 10.5194/acp-17-705-2017, 2017.

Canonaco, F., Crippa, M., Slowik, J. G., Baltensperger, U., and Prévôt, A. S. H.: SoFi, an IGOR-based interface

https://doi.org/10.5194/acp-2020-11
Preprint. Discussion started: 28 February 2020
© Author(s) 2020. CC BY 4.0 License.

Atmospheric Chemistry and Physics Discussions

for the efficient use of the generalized multilinear engine (ME-2) for the source apportionment: ME-2 application to aerosol mass spectrometer data, Atmospheric Measurement Techniques, 6, 3649-3661, 10.5194/amt-6-3649-2013, 2013.

Cao, X., Yao, Z., Shen, X., Ye, Y., and Jiang, X.: On-road emission characteristics of VOCs from light-duty gasoline vehicles in Beijing, China, Atmospheric Environment, 124, 146-155, https://doi.org/10.1016/j.atmosenv.2015.06.019, 2016.

Cappellin, L., Karl, T., Probst, M., Ismailova, O., Winkler, P. M., Soukoulis, C., Aprea, E., Märk, T. D., Gasperi, F., and Biasioli, F.: On quantitative determination of volatile organic compound concentrations using proton transfer reaction time-of-flight mass spectrometry, Environmental Science & Technology, 46, 2283-2290, 10.1021/es203985t, 2012.

Coggon, M. M., Lim, C. Y., Koss, A. R., Sekimoto, K., Yuan, B., Gilman, J. B., Hagan, D. H., Selimovic, V., Zarzana, K., Brown, S. S., Roberts, J. M., Müller, M., Yokelson, R., Wisthaler, A., Krechmer, J. E., Jimenez, J. L., Cappa, C., Kroll, J., de Gouw, J., and Warneke, C.: OH-chemistry of non-methane organic gases (NMOG) emitted from laboratory and ambient biomass burning smoke: evaluating the influence of furans and oxygenated aromatics on ozone and secondary NMOG formation, Atmos. Chem. Phys. Discuss., 2019, 1-42, 10.5194/acp-2019-516, 2019.

Crutzen, P. J., and Andreae, M. O.: Biomass Burning in the Tropics: Impact on Atmospheric Chemistry and Biogeochemical Cycles, Science, 250, 1669-1678, 10.1126/science.250.4988.1669, 1990.

de Gouw, J., and Warneke, C.: Measurements of volatile organic compounds in the earth's atmosphere using proton-transfer-reaction mass spectrometry, Mass Spectrom Rev, 26, 223-257, 10.1002/mas.20119, 2007.

de Gouw, J. A., Middlebrook, A. M., Warneke, C., Goldan, P. D., Kuster, W. C., Roberts, J. M., Fehsenfeld, F. C., Worsnop, D. R., Canagaratna, M. R., Pszenny, A. A. P., Keene, W. C., Marchewka, M., Bertman, S. B., and Bates, T. S.: Budget of organic carbon in a polluted atmosphere: Results from the New England Air Quality Study in 2002, Journal of Geophysical Research: Atmospheres, 110, doi:10.1029/2004JD005623, 2005.

Derwent, R. G., Jenkin, M. E., Utembe, S. R., Shallcross, D. E., Murrells, T. P., and Passant, N. R.: Secondary organic aerosol formation from a large number of reactive man-made organic compounds, Science of The Total Environment, 408, 3374-3381, https://doi.org/10.1016/j.scitotenv.2010.04.013, 2010.

Ehn, M., Thornton, J. A., Kleist, E., Sipilä, M., Junninen, H., Pullinen, I., Springer, M., Rubach, F., Tillmann, R., Lee, B., Lopez-Hilfiker, F., Andres, S., Acir, I.-H., Rissanen, M., Jokinen, T., Schobesberger, S., Kangasluoma, J., Kontkanen, J., Nieminen, T., Kurtén, T., Nielsen, L. B., Jørgensen, S., Kjaergaard, H. G., Canagaratna, M., Maso, M. D., Berndt, T., Petäjä, T., Wahner, A., Kerminen, V.-M., Kulmala, M., Worsnop, D. R., Wildt, J., and Mentel, T. F.: A large source of low-volatility secondary organic aerosol, Nature, 506, 476, 10.1038/nature13032, 2014.

Fischer, E. V., Jacob, D. J., Yantosca, R. M., Sulprizio, M. P., Millet, D. B., Mao, J., Paulot, F., Singh, H. B., Roiger, A., Ries, L., Talbot, R. W., Dzepina, K., and Pandey Deolal, S.: Atmospheric peroxyacetyl nitrate (PAN): a global budget and source attribution, Atmos. Chem. Phys., 14, 2679-2698, 10.5194/acp-14-2679-2014, 2014.

Fraser, M. P., Cass, G. R., and Simoneit, B. R. T.: Gas-Phase and Particle-Phase Organic Compounds Emitted from Motor Vehicle Traffic in a Los Angeles Roadway Tunnel, Environmental Science & Technology, 32, 2051-2060, 10.1021/es970916e, 1998.

https://doi.org/10.5194/acp-2020-11
Preprint. Discussion started: 28 February 2020
© Author(s) 2020. CC BY 4.0 License.

Atmospheric Chemistry and Physics Discussions

Gani, S., Bhandari, S., Seraj, S., Wang, D. S., Patel, K., Soni, P., Arub, Z., Habib, G., Hildebrandt Ruiz, L., and Apte, J. S.: Submicron aerosol composition in the world's most polluted megacity: the Delhi Aerosol Supersite study, Atmos. Chem. Phys., 19, 6843-6859, 10.5194/acp-19-6843-2019, 2019.

Graus, M., Muller, M., and Hansel, A.: High resolution PTR-TOF: quantification and formula confirmation of VOC in real time, J Am Soc Mass Spectrom, 21, 1037-1044, 10.1016/j.jasms.2010.02.006, 2010.

Hallquist, M., Wenger, J. C., Baltensperger, U., Rudich, Y., Simpson, D., Claeys, M., Dommen, J., Donahue, N. M., George, C., Goldstein, A. H., Hamilton, J. F., Herrmann, H., Hoffmann, T., Iinuma, Y., Jang, M., Jenkin, M. E., Jimenez, J. L., Kiendler-Scharr, A., Maenhaut, W., McFiggans, G., Mentel, T. F., Monod, A., Prévôt, A. S. H., Seinfeld, J. H., Surratt, J. D., Szmigielski, R., and Wildt, J.: The formation, properties and impact of secondary organic aerosol: current and emerging issues, Atmos. Chem. Phys., 9, 5155-5236, 10.5194/acp-9-5155-2009, 2009.

Hoque, R. R., Khillare, P. S., Agarwal, T., Shridhar, V., and Balachandran, S.: Spatial and temporal variation of BTEX in the urban atmosphere of Delhi, India, Science of The Total Environment, 392, 30-40, https://doi.org/10.1016/j.scitotenv.2007.08.036, 2008.

IPCC: Climate Change 2013: The Physical Science Basis, Contribution of Working Group I to the Fifth Assessment Report of the Intergovernmental Panel on Climate Change, edited by: Stocker, T. F., Qin, D., Plattner, G.-K., Tignor, M., Allen, S. K., Boschung, J., Nauels, A., Xia, Y., Bex, V., and Midgley, P. M., Cambridge University Press, Cambridge, UK and New York, USA, 2013.

Jordan, A., Haidacher, S., Hanel, G., Hartungen, E., Märk, L., Seehauser, H., Schottkowsky, R., Sulzer, P., and Märk, T. D.: A high resolution and high sensitivity proton-transfer-reaction time-of-flight mass spectrometer (PTR-TOF-MS), International Journal of Mass Spectrometry, 286, 122-128, 10.1016/j.ijms.2009.07.005, 2009.

Kampa, M., and Castanas, E.: Human health effects of air pollution, Environmental Pollution, 151, 362-367, https://doi.org/10.1016/j.envpol.2007.06.012, 2008.

Karl, T. G., Christian, T. J., Yokelson, R. J., Artaxo, P., Hao, W. M., and Guenther, A.: The Tropical Forest and Fire Emissions Experiment: method evaluation of volatile organic compound emissions measured by PTR-MS, FTIR, and GC from tropical biomass burning, Atmos. Chem. Phys., 7, 5883-5897, 10.5194/acp-7-5883-2007, 2007.

Klein, F., Pieber, S. M., Ni, H., Stefenelli, G., Bertrand, A., Kilic, D., Pospisilova, V., Temime-Roussel, B., Marchand, N., El Haddad, I., Slowik, J. G., Baltensperger, U., Cao, J., Huang, R.-j., and Prévôt, A. S. H.: Characterization of Gas-Phase Organics Using Proton Transfer Reaction Time-of-Flight Mass Spectrometry: Residential Coal Combustion, Environmental Science & Technology, 52, 2612-2617, 10.1021/acs.est.7b03960, 2018.

Kumar, P., Khare, M., Harrison, R. M., Bloss, W. J., Lewis, A. C., Coe, H., and Morawska, L.: New directions: Air pollution challenges for developing megacities like Delhi, Atmospheric Environment, 122, 657-661, https://doi.org/10.1016/j.atmosenv.2015.10.032, 2015.

Languille, B., Gros, V., Petit, J.-E., Honoré, C., Baudic, A., Perrussel, O., Foret, G., Michoud, V., Truong, F., Bonnaire, N., Sarda-Estève, R., Delmotte, M., Feron, A., Maisonneuve, F., Gaimoz, C., Formenti, P., Kotthaus, S., Haeffelin, M., and Favez, O.: Wood burning: A major source of Volatile Organic Compounds during wintertime in the Paris region, Science of The Total Environment, 135055, https://doi.org/10.1016/j.scitotenv.2019.135055, 2019.

https://doi.org/10.5194/acp-2020-11
Preprint. Discussion started: 28 February 2020
© Author(s) 2020. CC BY 4.0 License.

Atmospheric Chemistry and Physics Discussions

Lawrence, M. G., and Lelieveld, J.: Atmospheric pollutant outflow from southern Asia: a review, Atmos. Chem. Phys., 10, 11017-11096, 10.5194/acp-10-11017-2010, 2010.

Mahata, K. S., Rupakheti, M., Panday, A. K., Bhardwaj, P., Naja, M., Singh, A., Mues, A., Cristofanelli, P., Pudasainee, D., Bonasoni, P., and Lawrence, M. G.: Observation and analysis of spatiotemporal characteristics of surface ozone and carbon monoxide at multiple sites in the Kathmandu Valley, Nepal, Atmos. Chem. Phys., 18, 14113-14132, 10.5194/acp-18-14113-2018, 2018.

Meylan, W. M., and Howard, P. H.: Computer estimation of the Atmospheric gas-phase reaction rate of organic compounds with hydroxyl radicals and ozone, Chemosphere, 26, 2293-2299, https://doi.org/10.1016/0045-6535(93)90355-9, 1993.

Mohr, C., Lopez-Hilfiker, F. D., Zotter, P., Prévôt, A. S. H., Xu, L., Ng, N. L., Herndon, S. C., Williams, L. R., Franklin, J. P., Zahniser, M. S., Worsnop, D. R., Knighton, W. B., Aiken, A. C., Gorkowski, K. J., Dubey, M. K., Allan, J. D., and Thornton, J. A.: Contribution of Nitrated Phenols to Wood Burning Brown Carbon Light Absorption in Detling, United Kingdom during Winter Time, Environmental Science & Technology, 47, 6316-6324, 10.1021/es400683v, 2013.

Monks, P. S., Granier, C., Fuzzi, S., Stohl, A., Williams, M. L., Akimoto, H., Amann, M., Baklanov, A., Baltensperger, U., Bey, I., Blake, N., Blake, R. S., Carslaw, K., Cooper, O. R., Dentener, F., Fowler, D., Fragkou, E., Frost, G. J., Generoso, S., Ginoux, P., Grewe, V., Guenther, A., Hansson, H. C., Henne, S., Hjorth, J., Hofzumahaus, A., Huntrieser, H., Isaksen, I. S. A., Jenkin, M. E., Kaiser, J., Kanakidou, M., Klimont, Z., Kulmala, M., Laj, P., Lawrence, M. G., Lee, J. D., Liousse, C., Maione, M., McFiggans, G., Metzger, A., Mieville, A., Moussiopoulos, N., Orlando, J. J., O'Dowd, C. D., Palmer, P. I., Parrish, D. D., Petzold, A., Platt, U., Pöschl, U., Prévôt, A. S. H., Reeves, C. E., Reimann, S., Rudich, Y., Sellegri, K., Steinbrecher, R., Simpson, D., ten Brink, H., Theloke, J., van der Werf, G. R., Vautard, R., Vestreng, V., Vlachokostas, C., and von Glasow, R.: Atmospheric composition change – global and regional air quality, Atmospheric Environment, 43, 5268-5350, https://doi.org/10.1016/j.atmosenv.2009.08.021, 2009.

Müller, M., Graus, M., Wisthaler, A., Hansel, A., Metzger, A., Dommen, J., and Baltensperger, U.: Analysis of high mass resolution PTR-TOF mass spectra from 1,3,5-trimethylbenzene (TMB) environmental chamber experiments, Atmospheric Chemistry and Physics, 12, 829-843, 10.5194/acp-12-829-2012, 2012.

Nurmatov, U. B., Tagieva, N., Semple, S., Devereux, G., and Sheikh, A.: Volatile organic compounds and risk of asthma and allergy: a systematic review and meta-analysis of observational and interventional studies, Primary Care Respiratory Journal, 22, PS9, 10.4104/pcrj.2013.00010, 2013.

Paatero, P., and Tapper, U.: Positive matrix factorization: A non-negative factor model with optimal utilization of error estimates of data values, Environmetrics, 5, 111-126, 10.1002/env.3170050203, 1994.

Paatero, P.: The Multilinear Engine—A Table-Driven, Least Squares Program for Solving Multilinear Problems, Including the n-Way Parallel Factor Analysis Model, Journal of Computational and Graphical Statistics, 8, 854-888, 10.1080/10618600.1999.10474853, 1999.

Paatero, P., and Hopke, P. K.: Discarding or downweighting high-noise variables in factor analytic models, Analytica Chimica Acta, 490, 277-289, https://doi.org/10.1016/S0003-2670(02)01643-4, 2003.

Pallavi, Sinha, B., and Sinha, V.: Source apportionment of volatile organic compounds in the northwest Indo-Gangetic Plain using a positive matrix factorization model, Atmos. Chem. Phys., 19, 15467-15482, 10.5194/acp-19-15467-2019, 2019.

https://doi.org/10.5194/acp-2020-11
Preprint. Discussion started: 28 February 2020
© Author(s) 2020. CC BY 4.0 License.

Pieber, S. M., Kumar, N. K., Klein, F., Comte, P., Bhattu, D., Dommen, J., Bruns, E. A., Kılıç, D., El Haddad, I., Keller, A., Czerwinski, J., Heeb, N., Baltensperger, U., Slowik, J. G., and Prévôt, A. S. H.: Gas-phase composition and secondary organic aerosol formation from standard and particle filter-retrofitted gasoline direct injection vehicles investigated in a batch and flow reactor, Atmos. Chem. Phys., 18, 9929-9954, 10.5194/acp-18-9929-2018, 2018.

Sahu, L. K., and Saxena, P.: High time and mass resolved PTR-TOF-MS measurements of VOCs at an urban site of India during winter: Role of anthropogenic, biomass burning, biogenic and photochemical sources, Atmospheric Research, 164-165, 84-94, https://doi.org/10.1016/j.atmosres.2015.04.021, 2015.

Sahu, S. K., Beig, G., and Parkhi, N. S.: Emissions inventory of anthropogenic PM2.5 and PM10 in Delhi during Commonwealth Games 2010, Atmospheric Environment, 45, 6180-6190, https://doi.org/10.1016/j.atmosenv.2011.08.014, 2011.

Sharma, S. K., Mandal, T. K., Saxena, M., Rashmi, Rohtash, Sharma, A., and Gautam, R.: Source apportionment of PM10 by using positive matrix factorization at an urban site of Delhi, India, Urban Climate, 10, 656-670, https://doi.org/10.1016/j.uclim.2013.11.002, 2014.

Srivastava, A.: Source apportionment of ambient VOCS in Mumbai city, Atmospheric Environment, 38, 6829-6843, https://doi.org/10.1016/j.atmosenv.2004.09.009, 2004.

Srivastava, A., Sengupta, B., and Dutta, S. A.: Source apportionment of ambient VOCs in Delhi City, Science of The Total Environment, 343, 207-220, https://doi.org/10.1016/j.scitotenv.2004.10.008, 2005.

Stockwell, C. E., Veres, P. R., Williams, J., and Yokelson, R. J.: Characterization of biomass burning emissions from cooking fires, peat, crop residue, and other fuels with high-resolution proton-transfer-reaction time-of-flight mass spectrometry, Atmos. Chem. Phys., 15, 845-865, 10.5194/acp-15-845-2015, 2015.

Tiitta, P., Leskinen, A., Hao, L., Yli-Pirilä, P., Kortelainen, M., Grigonyte, J., Tissari, J., Lamberg, H., Hartikainen, A., Kuuspalo, K., Kortelainen, A. M., Virtanen, A., Lehtinen, K. E. J., Komppula, M., Pieber, S., Prévôt, A. S. H., Onasch, T. B., Worsnop, D. R., Czech, H., Zimmermann, R., Jokiniemi, J., and Sippula, O.: Transformation of logwood combustion emissions in a smog chamber: formation of secondary organic aerosol and changes in the primary organic aerosol upon daytime and nighttime aging, Atmos. Chem. Phys., 16, 13251-13269, 10.5194/acp-16-13251-2016, 2016.

Wagner, P., and Kuttler, W.: Biogenic and anthropogenic isoprene in the near-surface urban atmosphere — A case study in Essen, Germany, Science of The Total Environment, 475, 104-115, https://doi.org/10.1016/j.scitotenv.2013.12.026, 2014.

WHO, Ambient (outdoor) air pollution in cities database 2014, report, World Health Organization, Geneva, 2014.

Yao, Z., Shen, X., Ye, Y., Cao, X., Jiang, X., Zhang, Y., and He, K.: On-road emission characteristics of VOCs from diesel trucks in Beijing, China, Atmospheric Environment, 103, 87-93, https://doi.org/10.1016/j.atmosenv.2014.12.028, 2015.

Yokelson, R. J., Crounse, J. D., DeCarlo, P. F., Karl, T., Urbanski, S., Atlas, E., Campos, T., Shinozuka, Y., Kapustin, V., Clarke, A. D., Weinheimer, A., Knapp, D. J., Montzka, D. D., Holloway, J., Weibring, P., Flocke, F., Zheng, W., Toohey, D., Wennberg, P. O., Wiedinmyer, C., Mauldin, L., Fried, A., Richter, D., Walega, J., Jimenez, J. L., Adachi, K., Buseck, P. R., Hall, S. R., and Shetter, R.: Emissions from biomass burning in the Yucatan, Atmos. Chem. Phys., 9, 5785-5812, 10.5194/acp-9-5785-2009, 2009.

Yuan, Y., Zhao, X., Wang, S., and Wang, L.: Atmospheric Oxidation of Furan and Methyl-Substituted Furans

https://doi.org/10.5194/acp-2020-11
Preprint. Discussion started: 28 February 2020
© Author(s) 2020. CC BY 4.0 License.

Atmospheric Chemistry and Physics Discussions

Initiated by Hydroxyl Radicals, The Journal of Physical Chemistry A, 121, 9306-9319, 0.1021/acs.jpca.7b09741, 2017.

https://doi.org/10.5194/acp-2020-11
Preprint. Discussion started: 28 February 2020
© Author(s) 2020. CC BY 4.0 License.

Atmospheric Chemistry and Physics Discussions

Figure captions:

Fig. 1 Maps of the study region and the two sampling sites (from Google Maps). The black circle denotes the urban site at IITD and the black square the suburban site at MRIU.

Fig. 2 Temporal variations of CO, NO_x, analyzed VOC mixing ratio and temperature as well as the contributions of seven VOC families at the two sites.

Fig. 3 PMF results at IITD, showing (a) factor profiles (b) time series and (c) diurnal patterns. In (a), the left axis for each factor profile is the relative composition of each factor (i.e., horizontal sum is 1) and the right axis is the relative contribution of each factor to a given ion. Ions are colored based on the seven family classes, as described in Section 3.1. (b) Temporal evolution of resolved factors at IITD, together with external reference data, e.g NOx, CO, solar radiation and temperature. (c) Medians of diurnal cycles of factors at IITD, shaded with interquartile ranges as well as 10^{th} and 90^{th} percentiles.

Fig. 4 PMF results at MRIU, showing (a) factor profiles (b) time series, and (c) diurnal patterns. (a) Relative composition (left axis) and relative contribution (right axis) of each factor to a given ion. Ions are colored based on the seven family classes, as described in Section 3.1. (b) Temporal evolution of resolved factors at MRIU, together with external reference data, e.g NO_x, CO, solar radiation and temperature. (c) Medians of diurnal cycles of factors at MRIU, shaded with interquartile ranges as well as 10^{th} and 90^{th} percentiles.

Fig. 5 Comparisons of averaged factor diurnal patterns and factor profiles at the two sites. The left panel represents mean and median diurnal cycles at the two sites, and the right panel the factor profiles with the IITD spectrum on top and the MRIU spectrum on bottom, color coded by the VOC families described in Section 3.1.

Fig. 6 Comparisons of averaged factor diurnal patterns and factor profiles of SecVOC2 at IITD and SecVOC1 at MRIU. The dots in the left panel represent the mean values and the triangles the median values.

Fig. 7 (a, c) Diurnal patterns of factor mixing ratios at the two sites, color-coded by the six retrieved factors. (b, d) Diurnal patterns of the fractional contributions of the factors at the two sites.

Fig. 8 Explained variations of selected ions at the two sites, stacked such the sum is the total explained variation, color coded by the six factors (a) at IITD and (b) at MRIU. Missing ions at MRIU were excluded from PMF analysis due to low SNR.

Fig. 9 Diurnal cycles of selected marker ions, stacked with explained variations by each factor, and the red line representing the measured average concentrations. Tentative structures assigned to the individual ions are denoted in each figure.

https://doi.org/10.5194/acp-2020-11
Preprint. Discussion started: 28 February 2020
© Author(s) 2020. CC BY 4.0 License.

Atmospheric Chemistry and Physics Discussions

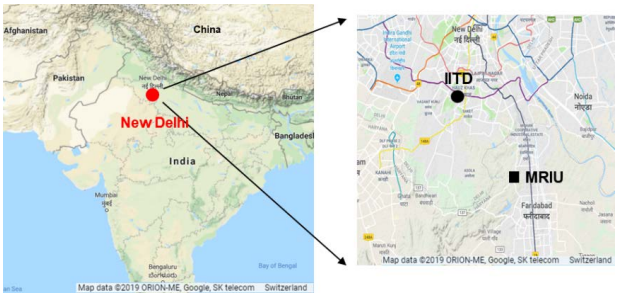

730 **Fig. 1** Maps of the study region and the two sampling sites (from © Google Maps). The black circle denotes the urban site at IITD and the black square the suburban site at MRIU.

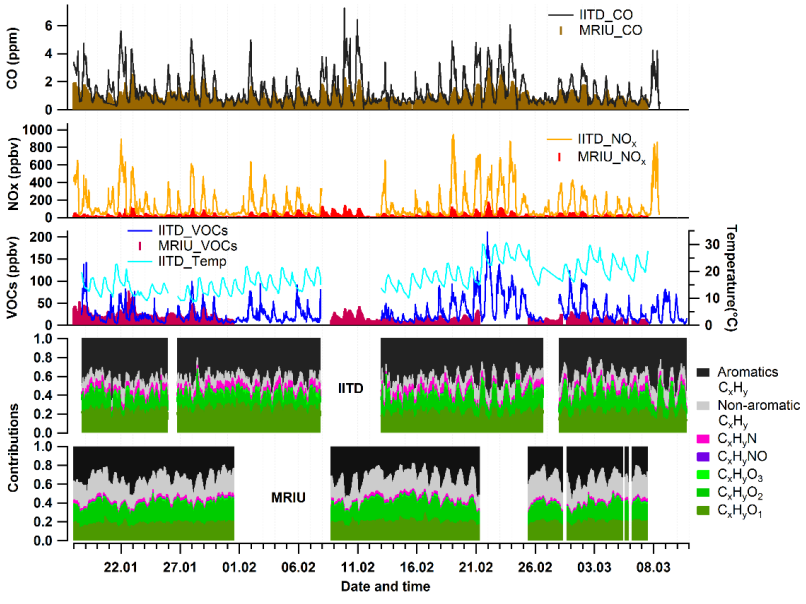

Fig. 2 Temporal variations of CO, NO_x, analyzed VOC mixing ratio and temperature as well as the contributions of seven VOC families at the two sites.

735

https://doi.org/10.5194/acp-2020-11
Preprint. Discussion started: 28 February 2020
© Author(s) 2020. CC BY 4.0 License.

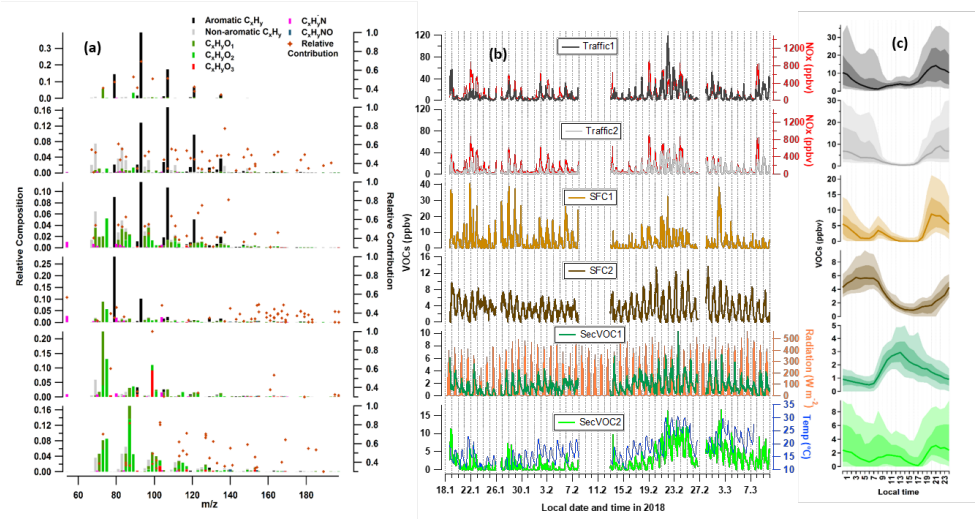

Fig. 3 PMF results at IITD, showing (a) factor profiles (b) time series and (c) diurnal patterns. In (a), the left axis for each factor profile is the relative composition of each factor (i.e., horizontal sum is 1) and the right axis is the relative contribution of each factor to a given ion. Ions are colored based on the seven family classes, as described in Section 3.1. (b) Temporal evolution of resolved factors at IITD, together with external reference data, e.g NO_x, CO, solar radiation and temperature. (c) Medians of diurnal cycles of factors at IITD, shaded with interquartile ranges as well as 10^{th} and 90^{th} percentiles.

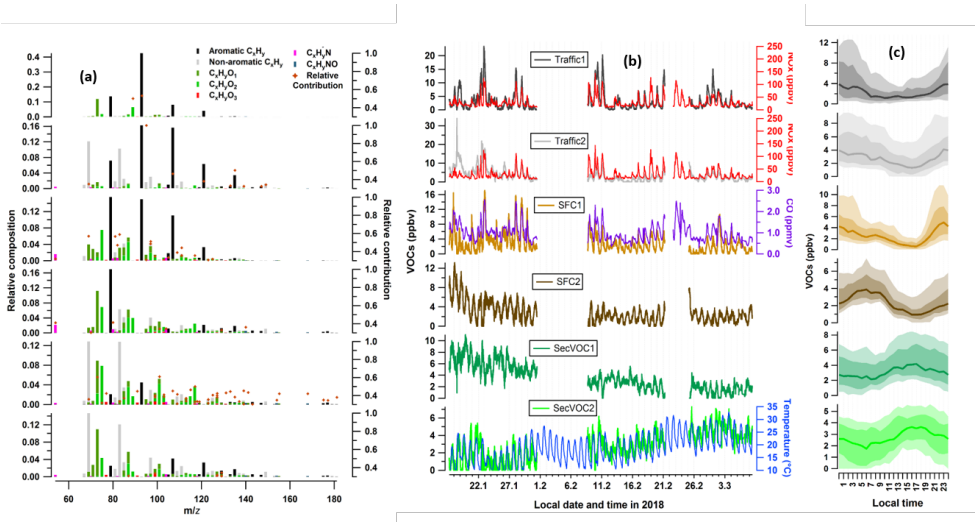

Fig. 4 PMF results at MRIU, showing (a) factor profiles (b) time series, and (c) diurnal patterns. (a) Relative composition (left axis) and relative contribution (right axis) of each factor to a given ion. Ions are colored based on the seven family classes, as described in Section 3.1. (b) Temporal evolution of resolved factors at MRIU,

https://doi.org/10.5194/acp-2020-11
Preprint. Discussion started: 28 February 2020
© Author(s) 2020. CC BY 4.0 License.

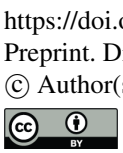

Atmospheric Chemistry and Physics Discussions

together with external reference data, e.g NO_x, CO, solar radiation and temperature. (c) Medians of diurnal cycles of factors at MRIU, shaded with interquartile ranges as well as 10th and 90th percentiles.

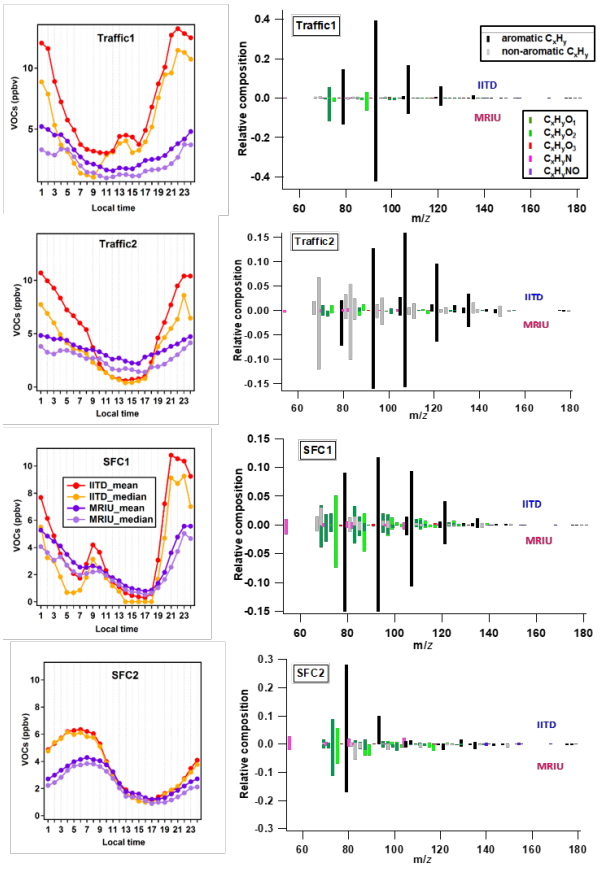

Fig. 5 Comparisons of averaged factor diurnal patterns and factor profiles at the two sites. The left panel represents mean and median diurnal cycles at the two sites, and the right panel the factor profiles with the IITD spectrum on top and the MRIU spectrum on bottom, color coded by the VOC families described in Section 3.1.

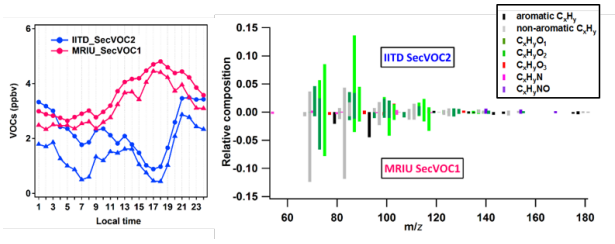

Fig. 6 Comparisons of averaged factor diurnal patterns and factor profiles of SecVOC2 at IITD and SecVOC1 at MRIU. The dots in the left panel represent the mean values and the triangles the median values.

https://doi.org/10.5194/acp-2020-11
Preprint. Discussion started: 28 February 2020
© Author(s) 2020. CC BY 4.0 License.

Atmospheric Chemistry and Physics Discussions

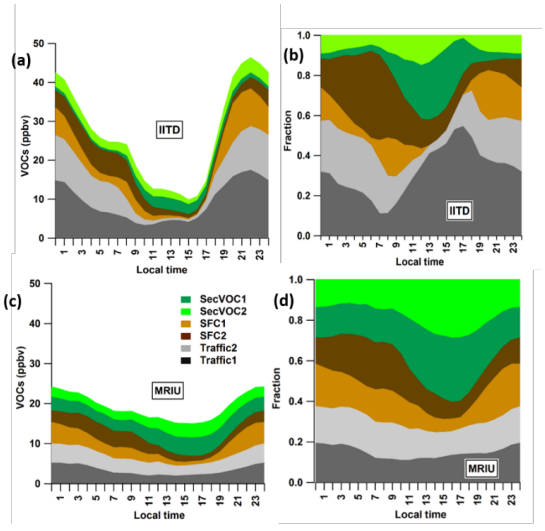

Fig. 7 (a, c) Diurnal patterns of factor mixing ratios at the two sites, color-coded by the six retrieved factors. (b, d) Diurnal patterns of the fractional contributions of the factors at the two sites.

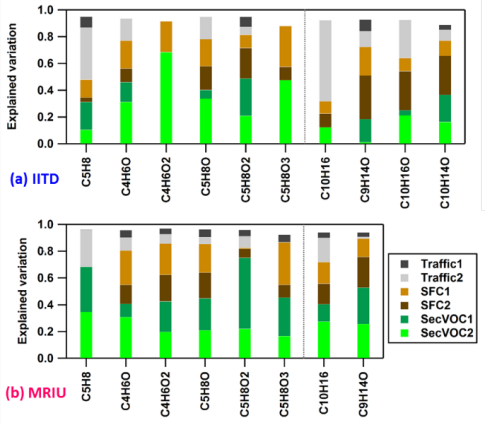

760

Fig. 8 Explained variations of selected ions at the two sites, stacked such the sum is the total explained variation, color coded by the six factors (a) at IITD and (b) at MRIU. Missing ions at MRIU were excluded from PMF analysis due to low SNR.

https://doi.org/10.5194/acp-2020-11
Preprint. Discussion started: 28 February 2020
© Author(s) 2020. CC BY 4.0 License.

Atmospheric Chemistry and Physics Discussions

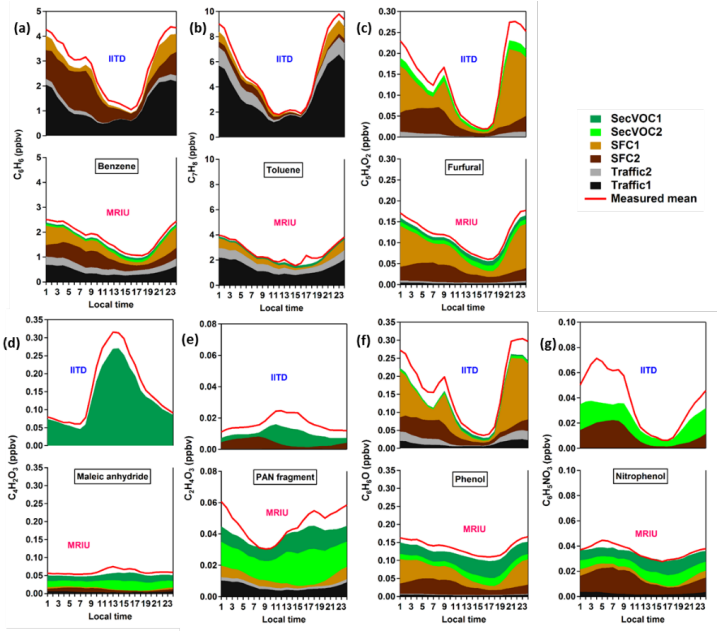

765 **Fig. 9** Diurnal cycles of selected marker ions, stacked with explained variations by each factor, and the red line representing the measured average concentrations. Tentative structures assigned to the individual ions are denoted in each figure.